A stellar origin for the short-lived nuclides in the early Solar System

S. Sahijpal*, J. N. Goswami*, A. M. Davis†, L. Grossman†‡ & R. S. Lewis†

** Physical Research Laboratory, Ahmedabad – 380 009, India*
† Enrico Fermi Institute, University of Chicago, 5640 South Ellis Avenue, Chicago, Illinois 60637, USA
‡ Department of the Geophysical Sciences, University of Chicago, 5734 South Ellis Avenue, Chicago, Illinois 60637, USA

Primitive meteorites contain isotopes that are the decay products of short-lived nuclides in the early Solar System[1,2]. The relative abundances of these isotopes provide a means to determine timescales for the formation and accretion of primitive Solar System objects, the abundances of the parent nuclides being fixed when these objects solidified. The abundances can also be used to investigate the source of the nuclides (such as ^{41}Ca, ^{26}Al, ^{60}Fe, ^{53}Mn and ^{107}Pd), although this is an area of controversy. The nuclides could have originated from a single stellar object[2–6], such as a nearby red-giant or a supernova. But observations of enhanced ion fluxes in a molecular cloud[7] have led to other models[8–10] in which these nuclides are formed by energetic particle irradiation of gas and dust in the protosolar molecular cloud; alternatively, irradiation by energetic particles from the active early Sun may have occurred within the solar nebula itself[11–18]. Here we show that there is a correlation between the initial abundances of ^{41}Ca and ^{26}Al in samples of primitive meteorite (as inferred from their respective decay products, ^{41}K and ^{26}Mg), implying a common origin for the short-lived nuclides. We can therefore rule out the mechanisms based on energetic particle irradiation, as they cannot produce simultaneously the inferred initial abundances of both nuclides. If, as our results suggest, a single stellar source is responsible for generating these nuclides, we can constrain to less than one million years the timescale for the collapse of the protosolar cloud to form the Sun.

We made the measurements of Mg and K isotope compositions in small domains (~10 μm) of refractory hibonite ($CaAl_{12-2x}Mg_xTi_xO_{19}$) grains present within Ca–Al-rich inclusions (CAIs) or as isolated fragments in three primitive meteorites. The main objectives of this study were to look for ^{26}Mg and ^{41}K excesses resulting from *in situ* decay of the two short-lived nuclides ^{41}Ca (mean life, $\tau \approx 0.15$ Myr) and ^{26}Al ($\tau \approx 1$ Myr) present at the time of formation of the hibonites and to test for a possible correlation between the amounts of these nuclides present in the early Solar System. The analysed samples include fragments of individual crystals and grains present in hibonite–spinel-rich refractory spherules from the CM chondrite Murchison, and grains present in CAIs found in two CV3 chondrites, Allende and Efremovka. Seven of the analysed hibonites were hand-picked from an HF–HCl insoluble residue of a large piece of the Murchison meteorite. An additional hibonite fragment (SH-7) was hand-picked from an exposed surface of Murchison and another sample (BB-4; a spherical hibonite–spinel-rich object) was recovered from the dense fraction of the powder produced by freeze–thaw disaggregation of another piece of Murchison. Polished sections of three hibonite-bearing CAIs (HAL and USNM 3529-42 from Allende and E50 from Efremovka) were also included in our study. The Mg and K isotopic measurements were carried out at the Physical Research Laboratory, Ahmedabad, India, with a high-

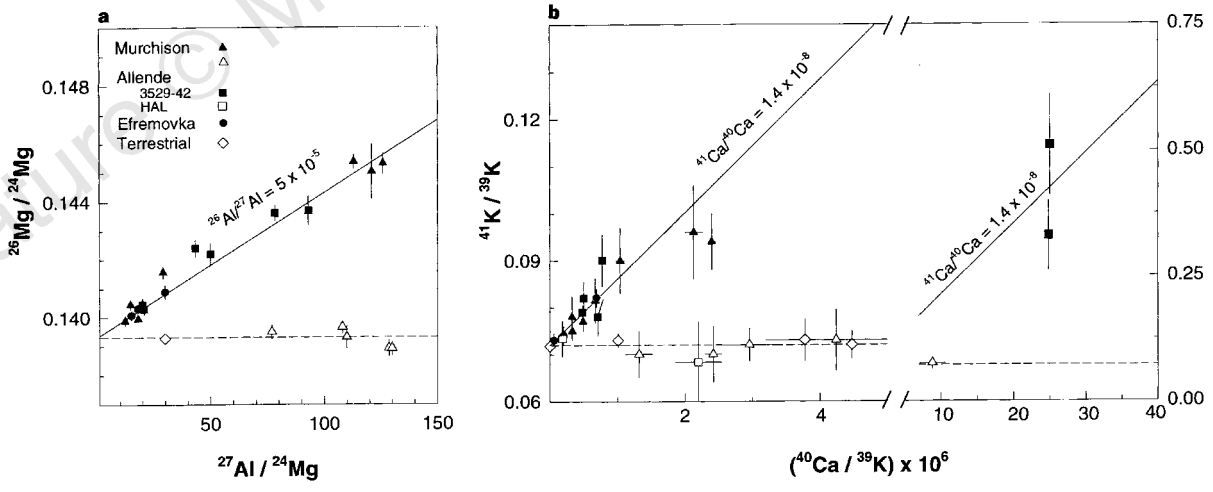

Figure 1 Magnesium and potassium isotopic compositions in hibonites from three primitive meteorites. Measured Mg and K isotopic ratios (^{26}Mg/^{24}Mg and ^{41}K/^{39}K) in meteoritic and terrestrial hibonites plotted as a function of their ^{27}Al/^{24}Mg and ^{40}Ca/^{39}K ratios, respectively (error bars are 1σ). **a**, Magnesium isotopic data from 12 analyses of Murchison hibonites, together with three from the Efremovka CAI E40 and six from the Allende CAI 3529-42. The filled symbols represent hibonites from these meteorites with excess ^{26}Mg (^{26}Mg/^{24}Mg > 0.13932); the open symbols represent hibonites devoid of measurable ^{26}Mg excess. Data for terrestrial hibonite are consistent with the reference Mg isotope ratio (^{26}Mg/^{24}Mg = 0.13932; the dashed horizontal line). The solid line represents the expected evolution of a closed Mg–Al system with initial ^{26}Al/^{27}Al of 5×10^{-5}. Mg–Al isotopic data for the Allende (HAL) hibonite[21] (not plotted) indicate high ^{27}Al/^{24}Mg ratio (>10^4) with a very low initial ^{26}Al/^{27}Al of ~5×10^{-8}. **b**, The K isotopic data; same symbols (filled or open) as in **a** are retained for representing the analysed hibonites. The larger error bars result from the low count rates at masses 39 and 41 due to the low K content (<1 p.p.m.) in the hibonites. The solid lines represent the expected evolution of a closed K–Ca isotope system with initial ^{41}Ca/^{40}Ca of 1.4×10^{-8}. The initial ^{41}Ca/^{40}Ca values for the three data sets with ^{41}K excess are $(1.41 \pm 0.58) \times 10^{-8}$ (Efremovka; three data points), $(1.09 \pm 0.34) \times 10^{-8}$ (Murchison hibonites; seven data points) and $(1.39 \pm 0.34) \times 10^{-8}$ (Allende 3529-42; six data points); errors are 2σ. Two analyses of Allende (HAL) hibonite did not reveal ^{41}K excess (open squares). Another measurement of HAL yielded ^{39}K count rate below our counting system background (0.01 c s^{-1}); we infer an upper limit for the initial ^{41}Ca/^{40}Ca from this analysis at 3×10^{-9} and a ^{40}Ca/^{39}K ratio of $> 2 \times 10^8$ (not plotted in the figure). The K isotopic ratios of the five Murchison hibonites devoid of ^{26}Mg excess and of terrestrial hibonite (Ca/K < 10^3) and pyroxene (Ca/K > 10^6) are consistent with the reference K isotopic ratio (^{41}K/^{39}K = 0.072; the dashed horizontal lines).

mass-resolution Cameca ims-4f secondary ion mass spectrometer using procedures described in detail elsewhere[19,20]. Measurement of the isotopic composition of Mg was followed by that of K at the same spot in each hibonite. In one case (HAL hibonite from Allende) we only measured the K isotope composition, as the Mg isotopic composition had been studied in detail earlier[21].

In Fig. 1, we show the measured Mg and K isotopic compositions in the analysed hibonites. The details of the data reduction procedure are described elsewhere[19]. We carried out multiple analysis of hibonites in the Allende and Efremovka CAIs, and in two of the larger Murchison samples. Single analysis of both Mg and K isotopic compositions was carried out in the other smaller ($< 50\,\mu m$) Murchison hibonites. The filled symbols in Fig. 1a represent hibonites from the three meteorites that have excess ^{26}Mg from *in situ* decay of ^{26}Al, the open symbols those devoid of any measurable excess. The measured $^{26}Mg/^{24}Mg$ ratio for terrestrial Madagascar hibonite is consistent with the reference value[22] of 0.13932. The solid line represents the expected evolution for a closed Al–Mg isotope system with an initial $^{26}Al/^{27}Al$ ratio of 5×10^{-5}, the commonly accepted initial abundance ratio at the time of formation of most of the CAIs[23]. In Fig. 1b, we show the results from the K isotope measurements. The data for terrestrial hibonite (and pyroxenes with high Ca/K ratios) are consistent with the reference $^{41}K/^{39}K$ ratio of 0.072 (ref. 24) represented by the dashed horizontal lines. The solid lines represent the expected evolution for a closed K–Ca isotope system with an initial $^{41}Ca/^{40}Ca$ of 1.4×10^{-8}, inferred from the data obtained from the study of the Efremovka CAIs[19,25].

The data presented in Fig. 1 show that hibonites with excess ^{26}Mg also have excess ^{41}K and this correlation holds on a microscopic ($\sim 10\,\mu m$) scale. Further, hibonites having excess ^{26}Mg and ^{41}K also have initial $^{26}Al/^{27}Al$ and $^{41}Ca/^{40}Ca$ ratios close to their characteristic early Solar System values of 5×10^{-5} and 1.4×10^{-8}, respectively[19,23]. We also note that when there is no excess ^{26}Mg corresponding to the decay of ^{26}Al (as in several Murchison hibonites), or when the inferred $^{26}Al/^{27}Al$ ratio is extremely low (for example in the Allende HAL hibonite[21]), we do not have any detectable ^{41}K excess. We therefore conclude that the abundances of the two short-lived nuclides ^{26}Al and ^{41}Ca in the early Solar System are intimately connected, indicating that they had a common origin. The absence of excess ^{26}Mg and ^{41}K in some of the hibonites may indicate a coupled heterogeneous distribution of these two nuclides in the solar nebula, or secondary processing that may have caused redistribution or exchange of both Mg and K isotopes in these cases leading to the observed normal isotopic compositions. There is petrographic evidence[26] for secondary processing in the case of the Allende CAI HAL, notably in the hibonite. However, it is difficult to draw specific conclusions in the case of the Murchison hibonites devoid of ^{26}Mg and ^{41}K excess, as the exact petrographic context of these hibonites, obtained by direct picking or acid dissolution of bulk meteorite samples, is unknown. The observed correlation between ^{26}Al and ^{41}Ca would be further substantiated if samples with a lower initial $^{26}Al/^{27}Al$ and well behaved Al–Mg systematics could be found, where one would not expect excess ^{41}K. For example, a sample with an initial $^{26}Al/^{27}Al$ value of $\sim 2.5 \times 10^{-5}$ would have an expected excess in ^{41}K below our detection limit. Unfortunately, none of the samples analysed either by us or others satisfy the requirements of both a low initial $^{26}Al/^{27}Al$ and a high Ca/K ratio necessary for K isotopic study.

The observed correlations between the two short-lived nuclides ^{26}Al and ^{41}Ca in refractory hibonite grains from primitive meteorites indicate that these two nuclides originated from a common source and followed the same pathways in the solar nebula before incorporation into these early Solar System solids. Although it is possible that both nuclides could have been produced during energetic particle irradiation either in a molecular cloud or in the early Solar System, we face the problem of matching the observed initial $^{26}Al/^{27}Al$ and $^{41}Ca/^{40}Ca$ abundances of 5×10^{-5} and 1.4×10^{-8}, respectively. Extensive calculations that consider production of ^{41}Ca, ^{26}Al, ^{53}Mn and ^{36}Cl by energetic particles within a molecular cloud complex[9,10], or by energetic particles emanating from an active early Sun and interacting with solar nebular gas[11–13,16] or early Solar System solids[13–15,18,27], clearly show that production of enough ^{26}Al to match the observed initial $^{26}Al/^{27}Al$ ratio will result in a value of $^{41}Ca/^{40}Ca$ more than an order of magnitude higher than observed. Overproduction of ^{53}Mn and ^{36}Cl by a similar magnitude is also predicted. One way to circumvent the problem of overproduction of the shorter-lived nuclide ^{41}Ca ($\tau \approx 0.15$ Myr) will be to invoke a time interval of a few times 10^5 years, between the cessation of production by energetic particles and the formation of the analysed hibonites, so that the abundance of ^{41}Ca goes down while that of ^{26}Al ($\tau \approx 1$ Myr) remains essentially unaffected. However, it is difficult to support such an *ad hoc* hypothesis and the problem of overproduction of the relatively longer-lived nuclide ^{53}Mn ($\tau = 5.3$ Myr) will remain.

On the other hand, specific models have been proposed to explain the observed initial $^{26}Al/^{27}Al$ and $^{41}Ca/^{40}Ca$ ratios in early Solar System objects in terms of the production rates of these nuclides in different stellar sources such as a thermally pulsing asymptotic giant branch (TP-AGB) star, a massive supernova or a Wolf–Rayet star[2–6,28]. The choice of the most probable stellar source is made difficult by the two free parameters involved in these models; the dilution of the freshly synthesized stellar material by material in the source region and later with protosolar cloud material, and the time interval between the injection of the freshly synthesized nuclides into the protosolar cloud and the formation of the early Solar System objects, such as the hibonites analysed in this work. However, if we consider the dilution factor to be similar for both ^{26}Al and ^{41}Ca, a TP-AGB star seems to be a likely candidate[19]. A final resolution of the most plausible stellar source of these nuclides will require a better understanding of the interactions of these stellar objects with their surroundings[2–6,28] as well as the dynamics of the eventual injection of freshly synthesized nuclides into the protosolar cloud, an event that could have triggered its collapse[29,30].

In conclusion, our data do not support the proposals that energetic particle interactions within the protosolar molecular cloud or later in the solar nebula led to the production of the short-lived nuclides ^{26}Al and ^{41}Ca present in the early Solar System. Of course, we cannot completely rule out any contribution from this process; but if it is there, it must be at a much lower level than the contribution from the stellar source and may be ignored. Although the stellar source for the short-lived nuclides in the early Solar System cannot be identified unambiguously, a stellar origin for these nuclides, and particularly for ^{41}Ca with a mean life of 0.15 Myr, constrains the timescale for the collapse of the protosolar cloud to form the Sun and some of the first Solar System objects to less than a million years[4,5,19,28,31]. □

Received 29 May; accepted 14 November 1997.

1. Waserburg, G. J. in *Protostars and Planets II* (eds Black, D. C. & Matthews, M. S.) 703–737 (Univ. Arizona Press, Tucson, 1985).
2. Cameron, A. G. W. in *Protostars and Planets III* (eds Levy, E. H. *et al.*) 47–73 (Univ. Arizona Press, Tucson, 1993).
3. Wasserburg, G. J., Busso, M., Gallino, R. & Raiteri, C. M. Asymptotic Giant Branch Stars as a source of short-lived radioactive nuclei in the solar nebula. *Astrophys. J.* **424,** 412–428 (1994).
4. Wasserburg, G. J., Gallino, R., Busso, M., Goswami, J. N. & Raiteri, C. M. Injection of freshly synthesized ^{41}Ca in the early solar nebula by an asymptotic giant branch star. *Astrophys. J. Lett.* **440,** L101–L104 (1995).
5. Cameron, A. G. W., Höflich, P., Myers, P. C. & Clayton, D. D. Massive supernova, Orion gamma rays and the formation of the solar system. *Astrophys. J. Lett.* **447,** L53–L57 (1995).
6. Arnould, M., Paulus, G. & Meynet, G. Short-lived radionuclide production by non-exploding Wolf–Rayet stars. *Astron. Astrophys* **321,** 452–465 (1997).
7. Bloemen, H. *et al.* COMPTEL observations of the Orion complex: Evidence for cosmic-ray induced gamma ray lines. *Astron. Astrophys.* **281,** L5–L8 (1994).
8. Clayton, D. D. Production of ^{26}Al and other extinct radionuclides by low-energy heavy cosmic rays in molecular clouds. *Nature* **368,** 222–224 (1994).
9. Clayton, D. D. & Jin, L. Gamma rays, cosmic rays, and extinct radioactivity in molecular cloud. *Astrophys. J.* **451,** 681–699 (1995).
10. Ramaty, R., Kozlovsky, B. & Lingenfelter, R. E. Light isotopes, extinct radioisotopes and gamma ray lines from low energy cosmic ray interactions. *Astrophys. J.* **456,** 525–540 (1996).
11. Heymann, D. & Dziczkaniec, M. Early irradiation of matter in the solar system: Magnesium (proton, neutron) scheme. *Science* **191,** 79–81 (1976).

12. Clayton, D. D., Dwek, E. & Woosley, S. E. Isotopic anomalies and proton irradiation in the early solar system. *Astrophys. J.* **214,** 300–315 (1977).
13. Heymann, D., Dziczkaniec, M., Walker, A., Huss, G. & Morgan, J. A. Effects of proton irradiation on a gas phase in which condensation take place. I. negative ^{26}Mg anomalies and ^{26}Al. *Astrophys. J.* **225,** 1030–1044 (1978).
14. Lee, T. A local proton irradiation model for isotopic anomalies in the solar system. *Astrophys. J.* **219,** 217–226 (1978).
15. Wasserburg, G. J. & Arnould, M. in *Lecture Notes in Physics 287, 4th Workshop on Nuclear Astrophysics* (eds Hillebrandt, W. *et al.*) 262–276 (Springer, Heidelberg, 1987).
16. Clayton, D. D. & Jin, L. A new interpretation of ^{26}Al in meteoritic inclusions. *Astrophys. J. Lett.* **451,** L87–L91 (1995).
17. Shu, F. H., Shang, H. & Lee, T. Toward an astrophysical theory of chondrites. *Science* **271,** 1545–1552 (1996).
18. Shu, F. H., Shang, H., Glassgold, E. & Lee, T. X-rays and fluctuating X-wind from protostars. *Science* **277,** 1475–1479 (1997).
19. Srinivasan, G., Sahijpal, S., Ulyanov, A. A. & Goswami, J. N. Ion microprobe studies of Efremovka CAIs: II. Potassium isotope composition and ^{41}Ca in the early solar system. *Geochim. Cosmochim. Acta* **60,** 1823–1835 (1996).
20. Goswami, J. N., Srinivasan, G. & Ulyanov, A. A. Ion microprobe studies of Efremovka CAIs: I. Magnesium isotope composition. *Geochim. Cosmochim. Acta* **58,** 431–447 (1994).
21. Fahey, A. J., Goswami, J. N., McKeegan, K. D. & Zinner, E. K. ^{26}Al, ^{244}Pu, ^{50}Ti, REE, and trace element abundances in hibonite grains from CM and CV meteorites. *Geochim. Cosmochim. Acta* **51,** 329–350 (1987).
22. Cantanzaro, E. J., Murphy, T. J., Garner, E. L. & Shields, W. R. Absolute isotopic abundance ratios and atomic weights of magnesium. *J. Res. NBS* **70a,** 453–458 (1966).
23. MacPherson, G. J., Davis, A. M. & Zinner, E. K. The distribution of aluminum-26 in the early solar system—A reappraisal. *Meteoritics* **30,** 365–386 (1995).
24. Garner, E. L., Murphy, T. J., Gramlich, J. W., Paulsen, P. J. & Barnes, I. L. Absolute isotopic abundance ratios and the atomic weight of a reference sample of potassium. *J. Res. NBS* **79a,** 713–725 (1975).
25. Srinivasan, G., Ulyanov, A. A. & Goswami, J. N. ^{41}Ca in the early solar system. *Astrophys. J. Lett.* **431,** L67–L70 (1994).
26. Allen, J. M., Grossman, L., Lee, T. & Wasserburg, G. J. Mineralogy and petrography of HAL, an isotopically-unusual Allende inclusion. *Geochim. Cosmochim. Acta* **44,** 685–699 (1980).
27. Goswami, J. N., Marhas, K. K. & Sahijpal, S. Production of short-lived nuclides by solar energetic particles in the early solar system (Abstr.). *Lunar Planet. Sci.* **XXVIII,** 439–440 (1997).
28. Arnould, M., Meynet, G. & Paulus, G. in *Astrophysical Implications of the Laboratory Study of Presolar Materials* (eds Bernatowicz, T. & Zinner, E.) 179–202 (AIP Press, New York, 1997).
29. Boss, A. P. & Foster, P. N. in *Astrophysical Implications of the Laboratory Study of Presolar Materials* (eds Bernatowicz, T. & Zinner, E.) 649–664 (AIP Press, New York, 1997).
30. Cameron, A. G. W., Vanhala, H. & Hölflich, P. in *Astrophysical Implications of the Laboratory Study of Presolar Materials* (eds Bernatowicz, T. & Zinner, E.) 665–696 (AIP Press, New York, 1997).
31. Cameron, A. G. W. The first ten million years in the solar nebula. *Meteoritics* **30,** 133–161 (1995).

Acknowledgements. We are grateful to G. J. Wasserburg, G. J. MacPherson and A. A. Ulyanov for providing the samples of Allende and Efremovka CAIs for our study. We also thank E. J. Olsen of the Field Museum of Natural History for specimens of Murchison and Allende from which SH-7, BB-4, HAL and the seven hand-picked grains were extracted. We appreciate comments received from A. G. W. Cameron and E. Zinner. We acknowledge support from the Department of Space, Government of India (S.S. and J.N.G.) and from the National Aeronautics and Space Administration (A.M.D., L.G. and R.S.L.). J.N.G. also acknowledges hospitality provided by the Lunar and Planetary Institute, Houston, during the preparation of this manuscript.

Correspondence and requests for materials should be addressed to J. N. Goswami (e-mail: goswami@prl.ernet.in).

Softening of nanocrystalline metals at very small grain sizes

Jakob Schiøtz, Francesco D. Di Tolla* & Karsten W. Jacobsen

Center for Atomic-scale Materials Physics and Department of Physics, Technical University of Denmark, DK2800 Lyngby, Denmark

Nanocrystalline solids, in which the grain size is in the nanometre range, often have technologically interesting properties such as increased hardness and ductility. Nanocrystalline metals can be produced in several ways, among the most common of which are high-pressure compaction of nanometre-sized clusters and high-energy ball-milling[1–4]. The result is a polycrystalline metal with the grains randomly orientated. The hardness and yield stress of the material typically increase with decreasing grain size, a phenomenon known as the Hall–Petch effect[5,6]. Here we present computer simulations of the deformation of nanocrystalline copper, which show a softening with grain size (a reverse Hall–Petch effect[3,7]) for the smallest sizes. Most of the plastic deformation is due to a large number of small 'sliding' events of atomic planes at the grain boundaries, with only a minor part being caused by dislocation activity in the grains; the softening that we see at small grain sizes is therefore due to the larger fraction of atoms at grain boundaries. This softening will ultimately impose a limit on how strong nanocrystalline metals may become.

To simulate the behaviour of nanocrystalline metals with the computer, we construct nanocrystalline 'samples' with structures similar to those observed experimentally: essentially equiaxed dislocation-free grains separated by narrow straight grain boundaries[1]. Each sample contains 8–64 grains in a 10.6-nm cube of material, resulting in grain sizes from 3.3 to 6.6 nm. The grains are produced by a Voronoi construction[8]: a set of grain centres are chosen at random, and the part of space closer to a given centre than to any other centre is filled with atoms in an f.c.c. (face-centred cubic) lattice with a randomly selected crystallographic orientation. A typical 'sample' is shown in Fig. 1a. To mimic the system's being deep within the bulk of a large sample, the system is replicated infinitely in all three spatial directions (periodic boundary conditions). The forces between the atoms are calculated with the effective-medium theory[9,10], which suitably describes many-atom interactions in metals. The metal chosen for these simulations is copper; very similar results were obtained with palladium. Before deforming the system we 'anneal' it by running a 50-ps molecular dynamics simulation at 300 K, allowing unfavourable configurations in the grain boundaries to relax. Doubling the duration of annealing does not have any significant effect, nor does an increase in the temperature to 600 K.

The main part of the simulation is a slow uniaxial deformation while minimizing the energy with respect to all atomic coordinates. The deformation is applied by expanding the simulation cell in one direction, while the size is allowed to relax in the two perpendicular directions.

The initial and final configurations of such a simulation with a total strain of 10% are shown in Fig. 1. We see how the grain boundaries have become thicker, indicating that significant activity has taken place there. In the grains a few stacking faults have appeared. They are the signature of dislocation activity within the grains.

To facilitate the analysis of the simulations, we identify which atoms are located at grain boundaries and which are inside the grains, by determining the local crystalline order[11,12]. Atoms in local f.c.c. order are considered to be 'inside' the grains; atoms in local h.c.p. (hexagonal close-packed) order are classified as stacking faults. All other atoms are considered as belonging to the grain boundaries. Unlike conventional materials, where the volume occupied by the grain boundaries is very small, a significant fraction (30–50%) of the atoms are in the grain boundaries, in agreement with theoretical estimates[2].

As the deformation takes place, we calculate the average stress in the sample as a function of the amount of deformation. For each grain size we simulated the deformation of seven different initial configurations. Figure 2a shows the obtained average deformation curves. We see a linear elastic region with a Young's modulus around 90–105 GPa (increasing with increasing grain size), compared with 124 GPa in macrocrystalline Cu (ref. 13). This is caused by the large fraction of atoms in the grain boundaries having a lower Young's modulus[14,15]. A similar reduction is seen in simulations where the nanocrystalline metal is grown from a molten phase[16]. The elastic region is followed by plastic yielding at around 1 GPa, and finally the plastic deformation saturates at a maximal flow stress around 3 GPa. The theoretical shear stress of a perfect single crystal is approximately 6 GPa for the potential used.

The main deformation mode is illustrated in Fig. 3b, where the relative motions of the atoms is shown. We see that most of the deformation occurs in the grain boundaries in the form of a large number of small sliding events, where only a few atoms (or sometimes a few tens of atoms) move with respect to each other. Occasionally a partial dislocation is nucleated at a grain boundary and moves through a grain. Such events are responsible for a minor part of the total deformation, but in the absence of diffusion they are

* Present address: SISSA, Via Beirut 2-4, I-34014 Grignano (TS), Italy.